18TH WORLD CONFERENCE ON EARTHQUAKE ENGINEERING
WCEE2024
MILAN

MILAN, ITALY
30TH JUNE - 5TH JULY 2024

www.wcee2024.it

EXPERIMENTAL AND ANALYTICAL EVALUATION OF RC WALLS WITH CONCRETE RETROFIT OVERLAYS

A. Albright[1], I. Koutromanos[2], J. Murcia-Delso[3], M. Aliasghar-Mamaghani[4], B. Pulido[5]

[1] Graduate Student, Virginia Polytechnic Institute and State University, Blacksburg, Virginia

[2] Associate Professor, Virginia Polytechnic Institute and State University, Blacksburg, Virginia

[3] Associate Professor, Polytechnic University of Catalonia, Barcelona, Spain

[4] Postdoctoral Research Fellow, The University of Texas at Austin

[5] Graduate Student, Polytechnic University of Catalonia, Barcelona, Spain

Abstract: *This paper studies the effectiveness of concrete overlays as a retrofit technique for older, non-ductile RC wall construction. Experimental tests are being conducted on two wall specimens with a barbell section, with and without concrete overlays, representing a hypothetical eight-story building in California. The first, unretrofitted specimen has already been tested, while the second is to be tested in early December 2023. The goal of the overlay design is to maximize the inelastic deformability of the wall, by precluding the occurrence of shear failure before the development of significant flexural deformations. The paper also presents the recent enhancement of a truss-modeling approach for RC walls, to simulate the impact of concrete overlays on the cyclic response and explicitly account for the bond-slip behavior of the wall-to-overlay interfaces. The constitutive law describing the behavior of the interfaces is based on a recent formulation, with some necessary modifications to enable analysis of surface interfaces with both simplified and high-fidelity modeling approaches. The analytical method is then applied in analyses of the response of the retrofitted specimen under cyclic loading. The analysis indicates that the overlay is expected to significantly enhance the inelastic deformability of the wall, by delaying the occurrence of localized cracking in the web.*

1. Introduction

A number of reinforced concrete wall buildings located in the seismically active West Coast of the United States require seismic retrofit to ensure an adequate performance during earthquakes. A commonly employed retrofit technique involves the application of concrete overlays on the existing walls. The specific scheme provides the capability to increase both the shear and (if necessary) the flexural strength of a wall, and enhancing the inelastic deformability. The behavior of a retrofitted wall strongly depends on the force transfer along the wall-to-overlay interfaces. This is why the wall surface is typically roughened and provided with anchors before installation of the retrofit overlay. A major challenge for researchers and engineers is the lack of analytical tools for nonlinear analysis and design verification of walls including concrete retrofit overlays. Ideally, such tools should be capable of explicitly accounting for the force transfer across interfaces and the potential impact of localized damage on the interface regions. Of course, data from experimental tests is also necessary for the reliable calibration and validation of analytical tools.

This paper presents an investigation focused on the effectiveness of shotcrete (i.e., sprayable concrete) overlays as a retrofit technique for nonductile RC wall specimens. Two half-scale wall specimens were constructed on the Thomas M. Murray Structural Engineering Laboratory of the Virginia Polytechnic Institute and State University. The first specimen, tested in March 2023, is unretrofitted, while the second, to be tested in December 2023, is retrofitted through a one-sided shotcrete overlay. First, the configuration of the specimens is described, followed by a discussion of the test results for the first, unretrofitted specimen, which failed at a relatively low drift ratio due to the formation of a localized inclined crack in the web and a shear-compressive failure at the toe of the wall. An accurate and computationally efficient analysis approach, based on the nonlinear truss concept for reinforced concrete members, has been calibrated with the results of the first specimen. Subsequently, the analysis approach is enhanced with the capability to account for the shotcrete overlay and for the shear transfer between the overlay and the concrete substrate. The latter relies on an implementation of a modified version of a recent constitutive model, accounting for the cyclic shear behavior of reinforced concrete cold joints. Analyses for the retrofitted specimen indicate that the retrofit overlay can significantly enhance the inelastic deformability of the wall, by delaying the formation of localized cracks.

2. Description of Test Specimens

The specimens considered in this paper are cantilever, half-scale representations of the bottom two stories in a prototype eight-story wall building. The building represents design and construction practice in California between the mid-1950s and mid-1960s. A review of buildings from that era, conducted with the aid of a professional advisory panel consisting of structural engineers based in California, provided a range of values for reinforcing steel content, concrete and steel strengths and sectional dimensions. Based on this review, the sectional geometry selected for the specimens was that of a barbell wall, i.e. a section consisting of a pair of end pilasters (columns), with a thinner, very lightly reinforced web in-between. An additional reason why the barbell geometry was selected instead of a rectangular one was that it was considered more challenging in terms of application of retrofit overlays.

The specimens were anchored on the strong floor of the laboratory, and their length was aligned with the North-South direction. The consideration of a cantilever configuration for the bottom two stories corresponds to an effective seismic height equal to 25% of the building height. This value was close to the minimum value of effective seismic height obtained from dynamic analyses of prototype RC wall buildings by Panagiotou (2017). The pilasters in the prototype wall had vertical and transverse reinforcement ratios of 3% and 0.25%, respectively, while the web was very lightly reinforced, with a value of 0.25% for both the horizontal and vertical reinforcement ratios. The concrete had a nominal strength of 3.5 ksi (24 MPa), while the steel of intermediate grade, corresponding to a yield stress of 40 ksi (275 MPa). Due to the fact that it was not possible to obtain grade 40 reinforcing steel, the vertical bars in the pilaster were using grade 60 steel, i.e. with a nominal yield stress of 60 ksi (413 MPa), while the transverse pilaster and web reinforcement consisted of D5 bars, i.e. bars with a sectional area of 0.05 in^2 (32 mm^2), which is practically identical to that of #2 bars. The expected yield strength of the D5 bars was equal to about 67 ksi (461 MPa). To satisfy similitude requirements for the specimens given the different yield strength of the actual reinforcement compared to that of the prototype structure, the specimen reinforcement quantities were so established to ensure that all products of $\rho \cdot f_y$, where ρ is the reinforcing steel ratio and f_y is the yield stress, were identical for the prototype wall and actual test specimens. The concrete used in the specimens had a maximum aggregate size of 0.5 in. (13 mm), aimed to roughly correspond to a half-scale representation of the concrete in the prototype structure. The actual compressive strength on the day of testing of Specimen 1, obtained from tests on cylindrical specimens, was 4.22 ksi (29 MPa. The average yield strength of the Grade 60 reinforcement was 71 ksi (489 MPa), while that of the D5 bars was 79 ksi (544 MPa).

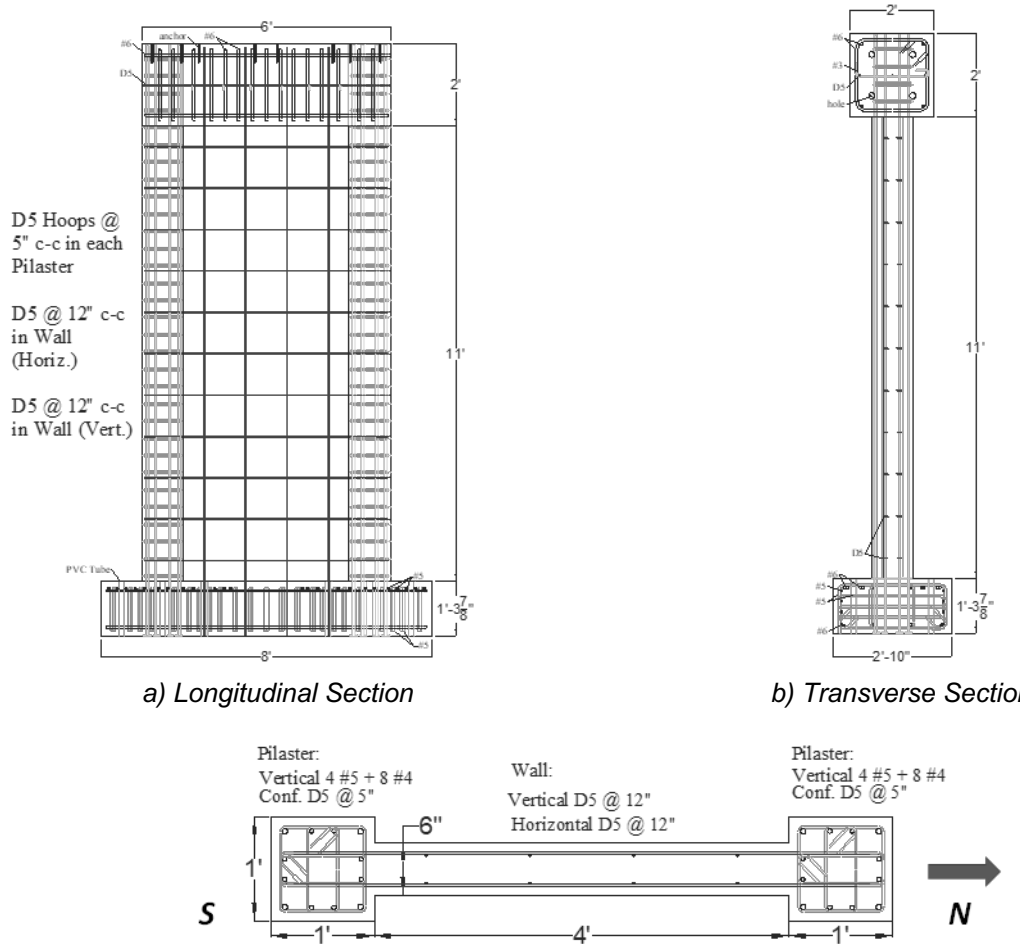

a) Longitudinal Section *b) Transverse Section*

c) Cross section

Figure 1. Configuration of Reinforced Concrete Wall (Note: 1 in. = 25.4 mm).

3. Test Results and Computational Analysis for Unretrofitted Specimen

The first specimen was subjected to a loading protocol consisting of a constant axial force of 200 kips (corresponding to an axial load ratio of approximately 10%), and a cyclic lateral force at the top. The axial force was applied through vertical prestressed rods, and care was taken to minimize the force in the rods during the test. The lateral force was applied through a servo-controlled hydraulic actuator. The test protocol initially included load-controlled cycles, followed by displacement-controlled cycles up to the occurrence of failure, i.e. significant strength degradation. Each level of force (for load-controlled cycles) or displacement (for displacement-controlled cycles) was pursued for two consecutive cycles. The load-controlled cycles targeted at a peak lateral force of 25 kip, 50 kip, 75 kip and 100 kip; the latter value was estimated to correspond to the cracking load of the wall. For both specimens, the final load-controlled cycles led to peak drift values of about 0.25%. Subsequently, the testing procedure was changed to a displacement-controlled one, with subsequent cycles targeting drift ratios of 0.50%, 0.75%, 1.00%, and 1.50%.

The hysteretic load-versus-drift curve obtained for the specimen is provided in Figure 2a, and the evolution of the cracking pattern is presented in Figure 2b. Multiple inclined cracks formed in the web and multiple horizontal cracks were obtained in the pilasters. As the lateral deformations increased, the width of several diagonal cracks in the web became bigger, and several horizontal bars had ruptured by the time the specimen had reached a drift ratio of 1%. Ultimately, the specimen incurred severe strength degradation at a drift ratio of about 1.3%, due to the formation of a strongly localized inclined crack in the web and a shear-crushing failure at the toe of the pilaster; a close-up view of the latter is shown in Figure 2c.

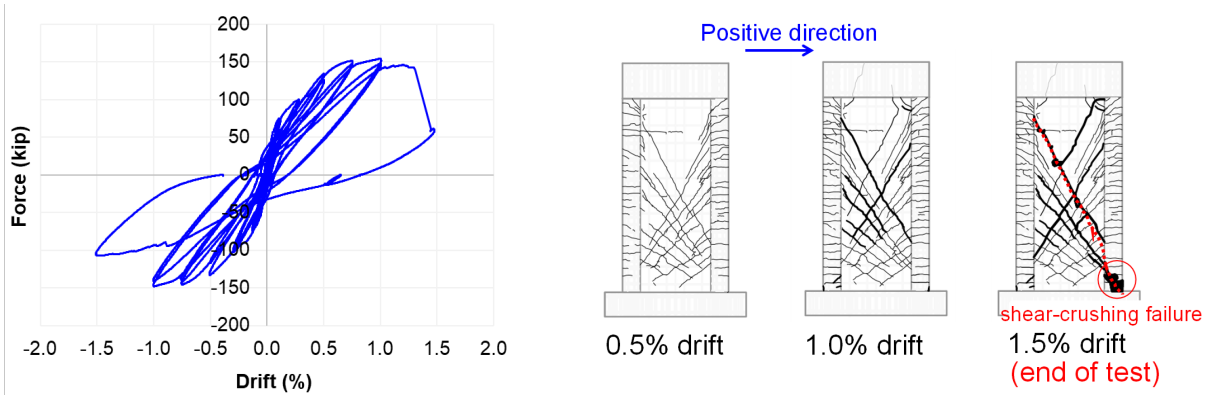

a) Load-deformation response b) Damage evolution

Figure 2. Summary Experimental Test Results for Unretrofitted Specimen 1

The experimental tests were accompanied with computational simulations, using the rectangular shell macroelement implementation of the nonlinear truss model described in detail in Deng et al. (2021). In the specific formulation a truss cell (consisting of two horizontal, two vertical and two inclined elements) is implemented as a 4-node rectangular element, as schematically summarized in Figure 3a, facilitating pre- and post-processing of analyses. The efficiency of the analytical approach is evidenced by the fact that it has enabled analyses of three-dimensional, multi-story, RC wall buildings, as shown in Figure 3b.

The analyses of the first specimen were performed twice, before and after the test. The pre-test analysis was meant to provide an estimate of the anticipated peak capacity and damage pattern. The peak-capacity prediction was necessary to ensure the adequacy of various test fixtures (reaction frames, base anchorage etc.). The comparison of the pre-test load-drift curve with the experimental observation is presented in Figure 4a. The same figure provides the maximum principal strain contour plot at the end of the pre-test analysis. The analysis was satisfactorily capable of predicting the final failure mode and the peak capacity. The latter was underestimated by 10%, due to the fact that the concrete compressive strength and Grade 60 reinforcement yield strength in the actual specimen were slightly higher than the values assumed in the analysis. A repetition of the truss analysis after the test, using the actual material strength values, gave a near-perfect match of the experimental damage pattern and load-displacement curve, as deduced from Figure 4b. These results, combined with results from analyses by Deng et al. (2021) for a set of experimental tests that encompassed all possible failure modes for walls, validate the predictive capability and accuracy of the employed analysis approach.

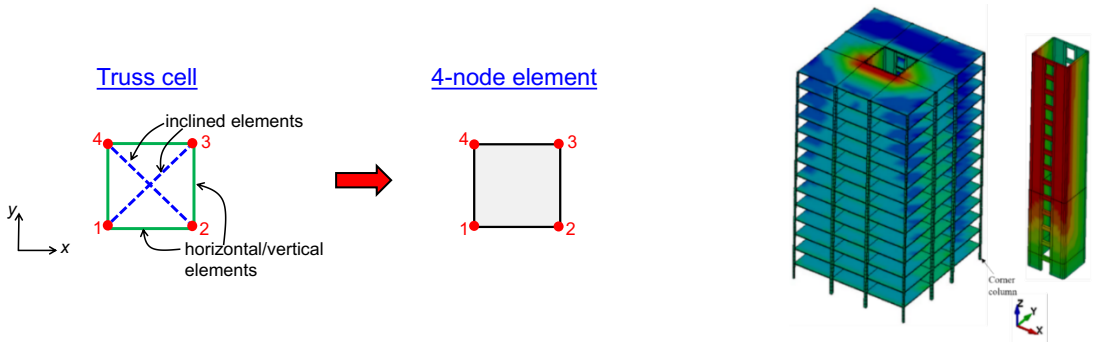

a) Modeling truss cell as rectangular macroelement (Deng et al. 2021) b) Analysis of RC core-wall building system (Mavros et al. 2022)

Figure 3. Computational modeling approach for wall specimens

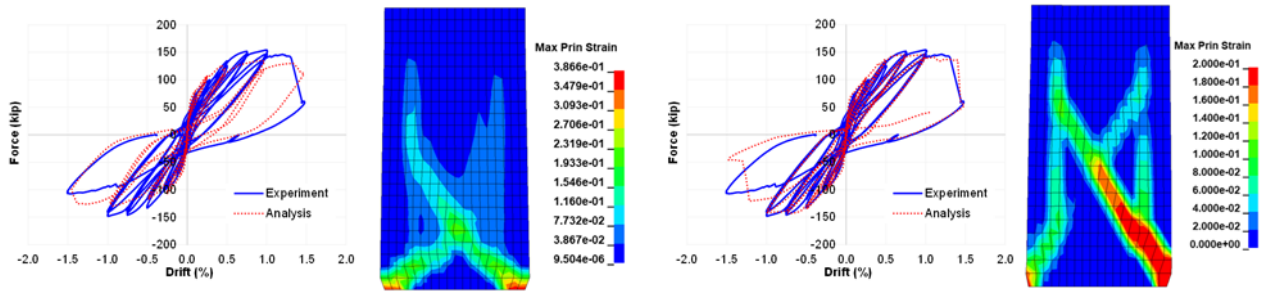

a) Pre-test analysis b) Post-test analysis

Figure 4. Results of Specimen 1 analysis using the nonlinear truss model

4. Design and Construction of Retrofitted Specimen

The cross-sectional geometry of the second, retrofitted specimen is presented in Figure 5a. The concrete overlay was designed to sufficiently increase the shear strength, without any change in the flexural strength, so that the wall would qualify as a flexure-dominated one per the ASCE 41-17 document (ASCE 2017). This was expected to preclude premature shear degradation before the wall develops significant flexural inelastic deformations. The specimen included a one-sided shotcrete overlay, with a thickness of 3 in. (76 mm) in the web region. The shotcrete mix was designed to pursue a compressive strength similar to that of the wall concrete. The overlay configuration was established based on input from the professional advisory panel, to represent the most common layout to be used for real-life buildings. The overlay included horizontal and vertical reinforcement, consisting of #3 bars (with a diameter of 9.5 mm) at a spacing of 9 inches (229 mm). This corresponds to an overlay reinforcing steel ratio of 0.41%. The horizontal bars were spliced with bars which were embedded inside the pilasters, as shown in Figure 5a, while the vertical bars were not anchored to the wall. As shown in the same figure, the surface of the web was roughened through a bushing tool, aimed to introduce a roughness of about ¼ in. (6 mm). D5 bar anchors were also installed in the web, by drilling holes up to a depth of 4 in. (102 mm). The drilled holes were filled with epoxy resin to ensure adequate anchorage strength. The horizontal and vertical spacing of the D5 anchors was 18 in. (457 mm) and 9 in. (229 mm), respectively. The shotcrete application process is shown in Figure 5b. The roughened surface of the web was sprayed with water before the shotcrete was applied.

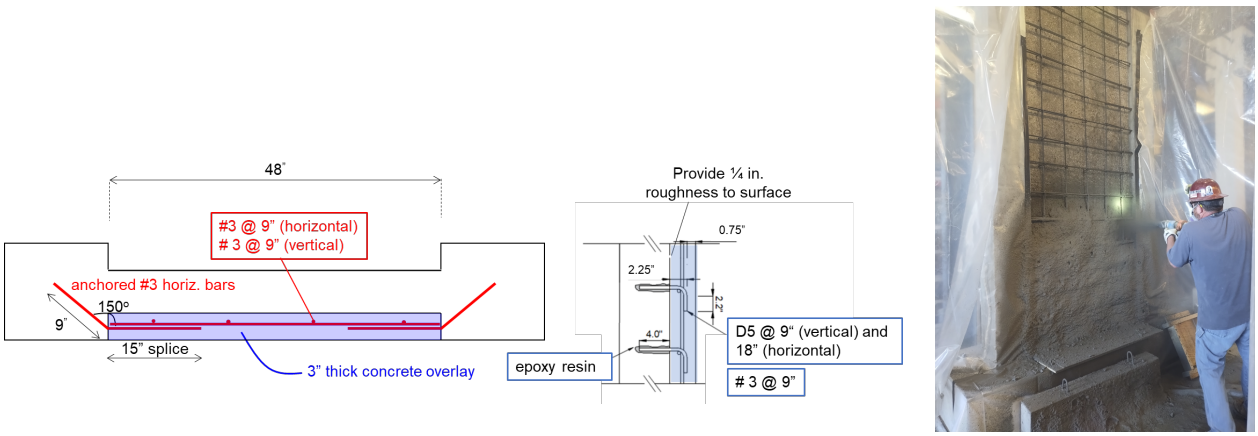

a) Design details b) Shotcrete application

Figure 5. Details and construction of Specimen 2 shotcrete overlay

5. Analysis of Retrofitted Specimen

An analysis using the truss modeling approach described above has been conducted for the retrofitted specimen. As shown in Figure 6a, the analysis approach was enhanced to explicitly account for the shotcrete overlay, by superimposing a layer of truss-shell macroelements on top of the part of the mesh representing the web of the wall. The possibility for relative slip between the overlay and the wall was modelled through zero-thickness, 8-node (surface) interface elements. The anchorage of the horizontal bars inside the wall pilasters was simulated through discrete, zero-length (spring) elements, as also shown in Figure 6a. The interface elements include three relative displacement components, as shown in Figure 6b, namely, a normal displacement component u_n, and two in-plane sliding components u_l and u_m, such that the three components are along three mutually perpendicular coordinate axes.

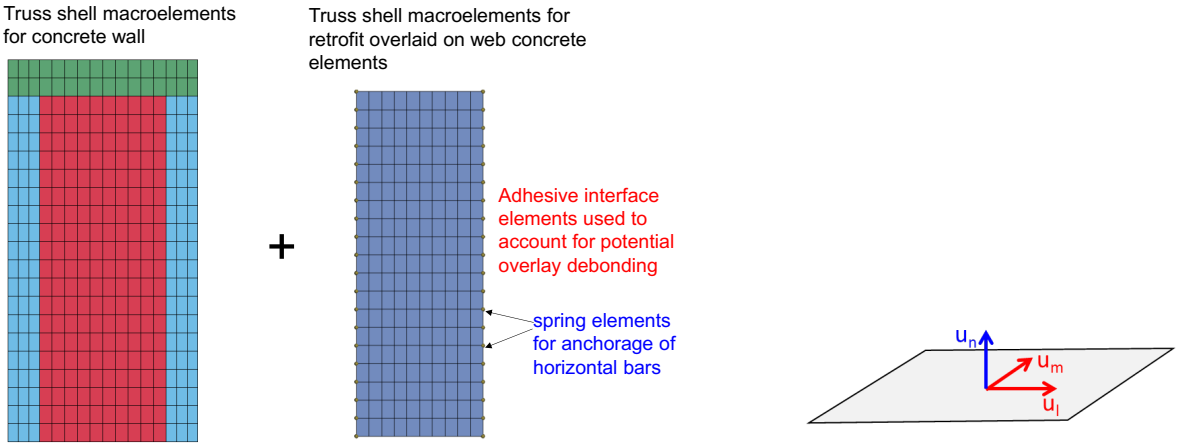

a) Nonlinear truss model b) Interface element local axes

Figure 6. Overview of computational modeling approach for walls with concrete retrofit overlays

The behavior of the interface between the overlay and the wall web is modeled using a modified version of the constitutive law for concrete interfaces by Palieraki et al. (2022). The specific law can phenomenologically describe the adhesive and frictional strength of interfaces such as cold joints, while also accounting for the impact of steel anchors on the shear transfer. The modifications pursued herein are not due to lack of accuracy in the original model (which was shown to have very good predictive capability), but to enable a model that can allow both the simplified representation of interfaces and can also be used in higher-fidelity models, e.g., three-dimensional continuum finite element models with discrete representation of the anchors through separate line elements (truss or beam elements).

The normal stress, σ_n, of the interface, is obtained from two contributions, i.e. the stress transferred by the concrete and the stress σ_s due to axial resistance of anchors. The concrete resistance is characterized by a normal stiffness parameter, D_{nn}. Given the normal displacement u_n of the interface, the total normal stress (positive when tensile) is given by:

$$\sigma_n = D_{nn}\left(u_n - u_g\right) - \rho_s \sigma_s \tag{1}$$

where ρ_s is the area ratio of the anchors (normalized anchor area over concrete tributary area), and u_g is the geometric, i.e. dilatational, part of the normal displacement, related to bulging accompanying shear sliding in rough interfaces which include asperities. Mode-I (tensile) fracture of the interface is accounted for through a linear tensile softening law shown in Figure 7a.

The tangential law is obtained by considering the overall tangential displacement, containing the combined effect of the two sliding displacement components, and then obtaining a corresponding tangential (shear) stress. The tangential displacement, u_t, is obtained from the two sliding displacement values, u_l and u_m:

$$u_t = \sqrt{u_l^2 + u_m^2} \tag{2}$$

The tangential stress σ_t is obtained as:

$$\sigma_t = D_{tt}\left(u_t - u_t^p\right) + \rho_s \tau_d \tag{3}$$

where u_t^p is the plastic part of the tangential displacement, D_{tt} is a tangential stiffness parameter, and τ_d is the shear stress in the anchors associated with dowel action (i.e., anchor dowel force divided by anchor sectional area). The dowel force D at each instant is a function of u_t in accordance with the law in Palieraki et al. (2022).

The yield strength, τ_y, for the tangential direction is obtained through a combination of cohesion and friction:

$$\tau_y = c + \mu \cdot \langle -\sigma_n \rangle \tag{4}$$

where c is a cohesive strength and μ is a dimensionless, frictional coefficient. The cohesive strength is a degrading function of the tangential plastic displacement, u_t^p, based on a linear softening law as presented in Figure 7b.

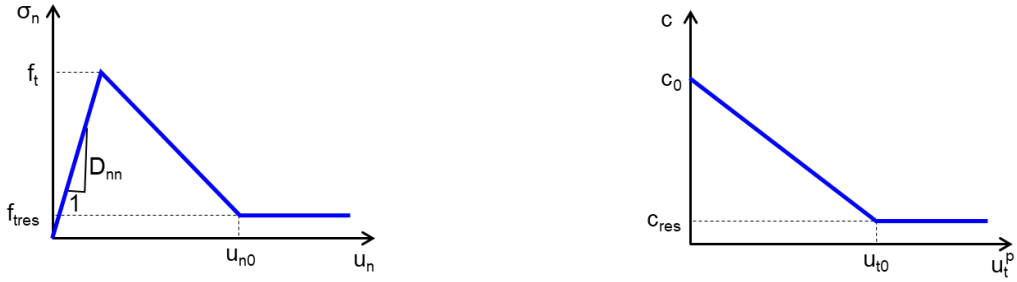

a) Normal tensile response b) Cohesive shear strength

Figure 7. Softening laws for interface elements

All that remains is to introduce the law that gives the geometric (dilatational) normal displacement of the interface as a function of the tangential displacement. The work by Palieraki et al. (2022) included a simple expression that connected the two quantities. However, the present work will adopt a different expression, based on the work of Puntel et al. (2006), which was deemed to be better-suited for description of concrete interfaces.

$$u_g(u_t) = f \cdot h_0 \left\{1 - \exp\left[-\frac{1}{2}\left(\frac{u_t}{s}\right)^2\right]\right\} \tag{5}$$

where h_0 and s are material constant parameters, essentially related to the size of the asperities on the joint, and f is an ever-decreasing integrity factor, accounting for the gradual smoothening of asperities with increasing shear inelastic work. The initial value of f in an analysis is 1, and its evolution is governed by the following rate equation (Puntel et al. 2006).

$$\dot{f} = -\max\left\{f_{\min}, \left\langle f - f_{asym} \right\rangle\right\} \cdot C_f \cdot \sigma_t \cdot \dot{u}_t \tag{6}$$

where f_{min} and C_f are material parameters and the value of f_{asym} is given by:

$$f_{asym} = \frac{1}{d \cdot \langle -\sigma_n \rangle + 1} \tag{7}$$

where d is another model parameter.

The axial and dowel action of anchors can be phenomenologically accounted for, essentially using the same equations as the ones in Palieraki et al. (2022). The only modification pertains to obtaining the axial stress of the anchors. The work by Palieraki et al. (2022) used the geometric normal displacement to obtain the corresponding stress. The present work adopts a different approach. The axial behavior of the anchors is assumed to be given by an elastic-perfectly plastic material model, after converting the geometric normal displacement to an axial strain ε_s. Maekawa et al. (2003) established an equation giving the relation between the ratio of u_g over d_b (d_b being the anchor diameter) and ε_s. This relation is inverted here to obtain:

$$\varepsilon_s = \frac{\sqrt{1+3500u_g / d_b} - 1}{3500} \tag{8}$$

Thus, the normal geometric displacement is converted to axial strain per Equation (8), then the axial strain is fed to the constitutive law to give the axial stress. This paper assumes an elastic-perfectly plastic law, characterized by the elastic modulus and yield stress of the actual bars used as anchors. The constitutive law only allows tensile axial stresses to be developed by the anchors.

The force-displacement response assumed for dowel action is the same as the one in Palieraki et al. (2022). The interaction between dowel action and axial resistance of the anchors is accounted for by enforcing the following inequality for the axial stress σ_s and the dowel stress τ_d (Palieraki et al. 2022).

$$\left(\frac{\sigma_s}{f_{sy}}\right)^{1.5} + \left(\frac{\tau_d}{\tau_{du}}\right)^{1.5} \leq 1 \tag{9}$$

where f_{sy} is the axial yield stress and τ_{du} is the ultimate dowel shear stress, given by the following expression.

$$\tau_{du} = \frac{D_u}{\pi \cdot d_b^2 / 4} \tag{10}$$

The value D_u is the ultimate dowel shear force that an anchor can carry, and is obtained from:

$$D_u = 1.3 d_b^2 \sqrt{f_{sy} \cdot f_c} \tag{11}$$

with f_c being the compressive strength of the concrete. Combining Equations (10) and (11) ultimately gives:

$$\tau_{du} = 1.65 \sqrt{f_{sy} \cdot f_c} \tag{12}$$

An analysis of the retrofitted specimen is conducted using the values c_o = 1 MPa, μ = 0.5, f_t = 0.5 MPa, h_0 = 1 mm and s = 1 mm. The analytically obtained load-displacement curves for the unretrofitted and retrofitted specimens are compared in Figure 8a. It can be seen that the retrofitted specimen is expected to reach significantly higher drift levels of about 2.0%, before the occurrence of strength degradation. The maximum principal strain contour plot at the instant of a positive drift ratio of 2.5%, shown in Figure 8b, indicates the ultimate formation of localized diagonal cracks in the center of the web, localized vertical cracks in the vicinity of the web-to-pilaster interfaces, and significant distortion in the vicinity of the toe of the pilaster. This distortion indicates that the ultimate damage pattern obtained for Specimen 1, marked in a circle in Figure 2b, will probably also occur in the retrofitted specimen. Figure 8c provides the contour plot of the magnitude of the relative slip (in mm) between the overlay and the concrete specimen at the end of the analysis. It can be seen that relatively large slip occurs in the vicinity of the vertical interfaces between the web and the pilasters, and in the middle portion of the wall length. The latter occurrence is related to the ultimate occurrence of diagonal cracking at the end of the analysis. The similarity of the ultimate failure modes for the unretrofitted and retrofitted walls indicates that the enhanced inelastic displacement capacity of the latter is due to the effectiveness of the concrete overlay in delaying the occurrence of localized cracks in the web.

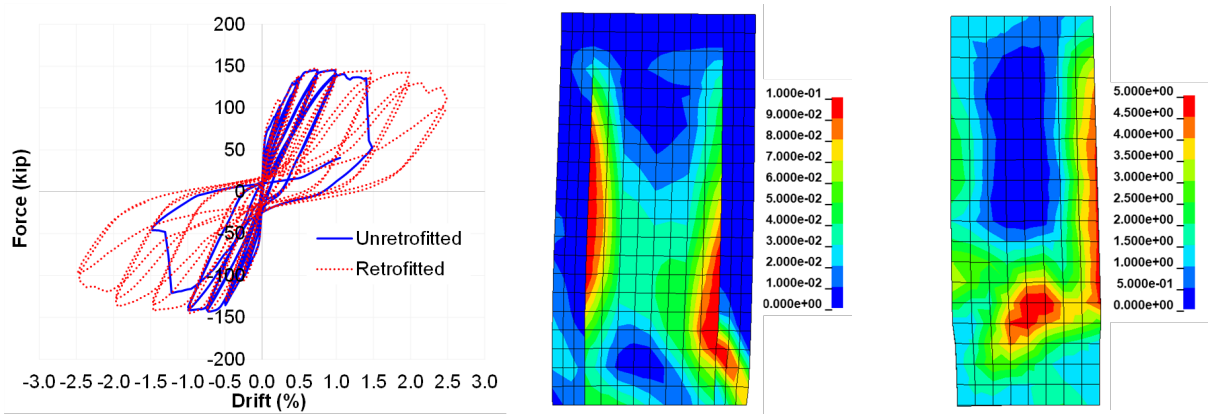

a) Load-displacement curves of unretrofitted and retrofitted specimens

b) Maximum principal strain contour at peak drift

c) Contour of slip (in mm) between overlay and wall concrete at end of analysis

Figure 8. Analysis results for retrofitted wall specimen

6. Conclusions

This paper has presented a study to investigate the effectiveness of shotcrete retrofit overlays in enhancing the seismic performance of non-ductile RC walls. The study constitutes a synergy of experimental testing and computational simulation. Two half-scale wall specimens, having a barbell section and representing detailing practice in California in the mid-1950s to mid-1960s, were constructed. The first specimen was unretrofitted and experienced shear-related strength degradation at a fairly low drift ratio. The second specimen, which is to be tested soon, includes a shotcrete overlay, specifically designed to prevent shear failure before the development of significant inelastic flexural deformations. Analyses have been conducted for the unretrofitted and retrofitted specimen, using a computationally efficient, truss modeling scheme, appropriately enhanced to account for the retrofit overlay and for the shear transfer across the interface between the overlay and the existing wall. The analyses indicate that the overlay will be expected to significantly enhance the ductility of the wall specimen, by delaying the occurrence of strongly localized cracks in the web.

7. Acknowledgements

The research presented in this paper was sponsored by the National Institute for Standards and Technology (NIST). The authors wish to acknowledge the help of the professional advisory panel in establishing the configuration of the tested specimens. The authors are also grateful to the Commercial Metals Company (CMC) and Headed Reinforcement Corporation (HRC) for donations of reinforcing steel for the specimens. Any opinions expressed in this paper are those of the authors alone and do not necessarily reflect the opinions of the sponsor, professional advisory panel and donors.

8. References

ASCE (2017). *ASCE 41-17: Seismic Evaluation and Retrofit of Existing Buildings*, American Society of Civil Engineers, Reston, VA.

Cortes-Puentes, L., and Palermo, D. (2012). “Modeling of RC Shear Walls Retrofitted with Steel Plates or FRP Sheets,” *ASCE Journal of Structural Engineering*, 138(5), 602-612.

Deng, X., Koutromanos, I., Murcia-Delso, J., and Panagiotou, M., (2021). “Nonlinear truss models for strain-based seismic evaluation of planar RC walls”, *Earthquake Engineering and Structural Dynamics*, 50(3), DOI: 10.1002/eqe.3480.

Maekawa, K., Pinanmas, A., Okamura, H. (2003). *Nonlinear Mechanics of Reinforced Concrete*, Spon Press, New York, NY.

Mavros, M., Panagiotou, M., Koutromanos, I., Alvarez, R., and Restrepo, J.I. (2022), “Seismic Analysis Of A Modern 14-Story RC Core Wall Building System Using The BTM-Shell Methodology,” *Earthquake Engineering and Structural Dynamics*, https://onlinelibrary.wiley.com/doi/epdf/10.1002/eqe.3627

Palieraki, V., Vintzileou, E., and Silva, J.F. (2022). “Modeling Reinforced Interfaces – Cold Joints Subjected to Cyclic Shear,” *ACI Structural Journal*, 119(4), 225-238.

Panagiotou, M. (2017). “Seismic Response of Medium-Rise and Tall RC Core-wall Buildings at Near-Fault Regions and Simplified Calculation of Design Demands,” *Proceedings of the 2017 Los Angeles Tall Buildings Structural Design Council*.

Puntel, E., Bolzon, G., and Saouma, V.E. (2006). “Fracture Mechanics Based Model for Joints Under Cyclic Loading,” *ASCE Journal of Engineering Mechanics*, 132(11), 1151-1159.